LBL-15294
Preprint c.2

Lawrence Berkeley Laboratory

UNIVERSITY OF CALIFORNIA

Materials & Molecular Research Division

RECEIVED
LAWRENCE
BERKELEY LABORATORY
MAY 17 1983
LIBRARY AND
DOCUMENTS SECTION

Submitted to the Journal of Vacuum Science and Technology

LEED AND AES STUDY OF STRUCTURAL AND CHEMISORPTIVE PROPERTIES OF Zr OVERLAYERS ON THE Pt(100) CRYSTAL FACE

U. Bardi, P.N. Ross, and G.A. Somorjai

March 1983

TWO-WEEK LOAN COPY

This is a Library Circulating Copy which may be borrowed for two weeks. For a personal retention copy, call Tech. Info. Division, Ext. 6782.

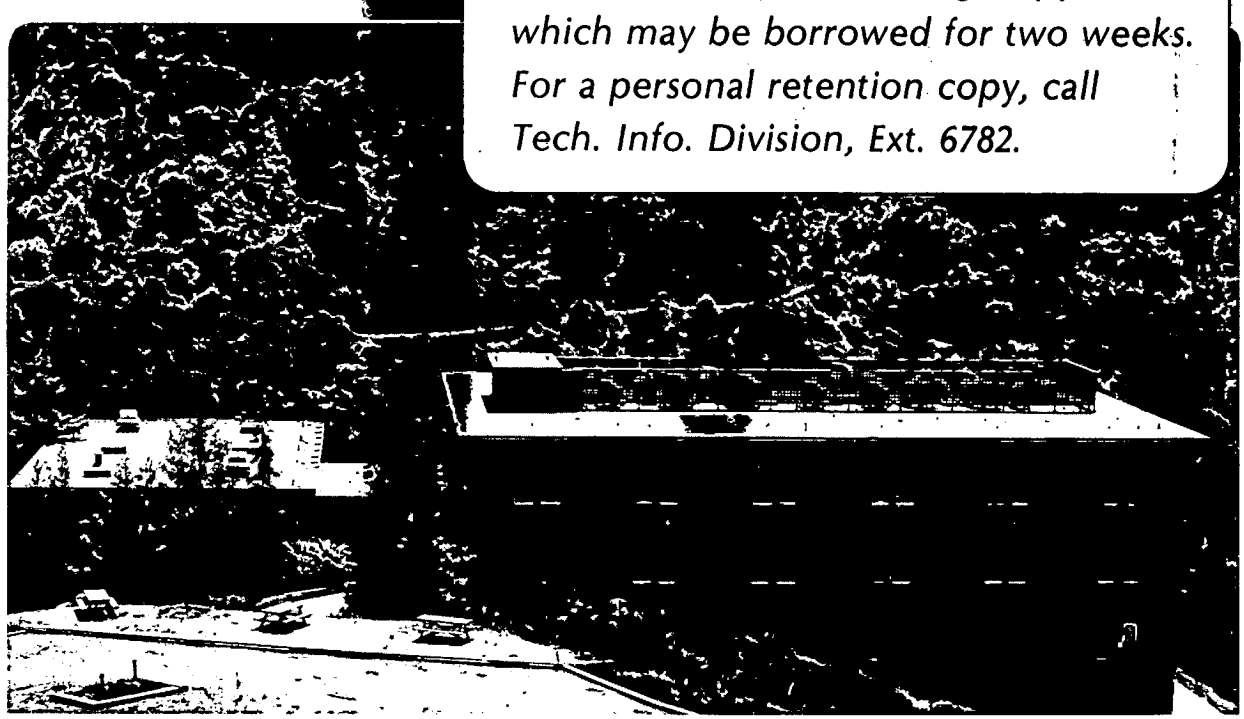

Prepared for the U.S. Department of Energy under Contract DE-AC03-76SF00098

LBL-15294 c.2

DISCLAIMER

This document was prepared as an account of work sponsored by the United States Government. While this document is believed to contain correct information, neither the United States Government nor any agency thereof, nor the Regents of the University of California, nor any of their employees, makes any warranty, express or implied, or assumes any legal responsibility for the accuracy, completeness, or usefulness of any information, apparatus, product, or process disclosed, or represents that its use would not infringe privately owned rights. Reference herein to any specific commercial product, process, or service by its trade name, trademark, manufacturer, or otherwise, does not necessarily constitute or imply its endorsement, recommendation, or favoring by the United States Government or any agency thereof, or the Regents of the University of California. The views and opinions of authors expressed herein do not necessarily state or reflect those of the United States Government or any agency thereof or the Regents of the University of California.

LBL-15294

LEED AND AES STUDY OF STRUCTURAL AND CHEMISORPTIVE PROPERTIES OF Zr OVERLAYERS ON THE Pt(100) CRYSTAL FACE

U. Bardi, P. N. Ross and G. A. Somorjai

Lawrence Berkeley Laboratory
Materials and Molecular Research Division
and
Department of Chemistry
University of California, Berkeley
Berkeley, California 94720

ABSTRACT

Zirconium overlayers were deposited onto a Pt(100) surface by electron beam evaporation in UHV, and the composition and structure of the surface was determined by AES and LEED. The overlayers were highly reactive towards oxygen, carbon monoxide and hydrocarbons, forming oxide or carbide overlayers. Several metastable ordered structures were observed by LEED when oxidized overlayers were thermally annealed in UHV. Protracted annealing at >900 K resulting in reduction and dissolution of the oxidized overlayer with complete disappearance of zirconium from the surface. Oxygen dosing of annealed surfaces at 25°C caused resegregation of zirconium to the surface, and the formation of an ordered Pt Zr_xO_y surface phase. This phase was stable in oxygen at 25-300°C, but oxygen dosing at above 300°C resulted in precipitation of ZrO_2 islands on top of the Pt(100)-(1x1) substrate.

1. INTRODUCTION

Platinum-zirconium intermetallic compounds are characterized by a highly exothermic heat of formation indicative of strong intermetallic bonding. According to Brewer (1), this strong bonding can be explained in terms of a valence-bond model which takes into account the interaction of the electrons in the d shell of both metals. In the framework of the regular solution theory (2) Zr - Pt alloys form an interesting limiting case, where the difference in the surface energy of the pure metals is small, and therefore the surface composition is controlled by the highly negative heat of formation of the alloys. Another reason for interest in the Pt/Zr system is related to recent developments in the field of catalysis. The Pt_3Zr alloy, together with other Pt-IVb intermetallics, has been reported (3) to show a higher catalytic activity than pure platinum in the electrolytic reduction of oxygen to water in acid fuel cells. A study of the surface properties of the Pt/Zr system would, therefore, be of both theoretical and technological interest.

We carried out our studies of the Pt-Zr system by depositing metallic zirconium on a (100) oriented single crystal Pt surface in ultra high vacuum. This method of preparation permitted us to vary the Zr/Pt atomic ratio on the surface and, therefore, to study the surface properties over a wide range of zirconium coverages. With the deposition procedure used here, zirconium overlayers grew on the Pt(100) surface by the layer-by-layer mechanism. Annealing at high temperatures (>900 K) caused dissolution of the Zr overlayer into the Pt bulk. Zirconium deposited on platinum was found to react readily with oxygen, carbon monoxide and hydrocarbons forming oxides and carbides. Annealing the

surface reduced the oxidation rate, but oxygen dosing of the annealed surface at high temperature and pressure appeared to produce the same surface phase regardless of the initial composition. Several ordered structures were found by LEED corresponding to different degrees of Zr coverage and degrees of oxidation of the Zr layer. The presence of these structures indicates that the Pt-Zr interaction remains strong even when zirconium is oxidized.

2. THERMODYNAMICS OF THE Pt-Zr SYSTEM

We summarize in this section the available thermodynamic data for the compounds which may form from the interaction of the metals and gases (O_2, CO) used in this study. Table 1 reports the free energies of formation for some compounds at 1273 K, the highest temperature obtainable in our experimental conditions. The Pt-Zr system has very negative free energies of formation for the binary alloys. However, ZrO_2 is the most stable of all Zr compounds. From the thermodynamic data, it is possible to calculate the equilibrium oxygen pressure for the reaction:

$$Pt_x\,Zr + O_2 \rightleftarrows Pt + ZrO_2$$

These equilibrium O_2 pressures are extremely low, so that in the presence of measurable (by conventional mass spectrometers) amounts of oxygen, all Pt-Zr alloys are unstable and will tend to show phase separation with formation of ZrO_2.

Under suitably reducing atmospheres, it can also be shown that Pt should reduce ZrO_2 and either dissolve Zr metal or form one of the intermetallics. In the case of H_2 as the reducing gas, the appropriate equilibrium is,

Table 1. Gibbs Free Energies of Formation at 1273 K.

Compound	ZrC	$ZrO_2(c)$	$H_2O(g)$	$CO_2(g)$	CO(g)	$Pt_3Zr(c)$	Dilute Alloy
ΔG_f^{1273}	-44	-203.5	-42.0	-94.7	-54.1	-92.1	-97
Ref.	13	13	13	13	13	12	12

$$Pt + ZrO_2 + 2\ H_2 \rightleftharpoons Pt_x\ Zr + 2\ H_2O$$

The equilibrium lies to the right as written for $\log(P_{H_2}/P_{H_2O}) > 3.6$ at 1273 K. In the case of CO as the reducing gas, the appropriate equilibrium is,

$$Pt + ZrO_2 + 2\ CO \rightleftharpoons Pt_x\ Zr + 2\ CO_2.$$

The equilibrium lies to the right as written for $\log\ (P_{CO}/P_{CO_2}) > 2.5$ at 1273 K. In the studies to be described here, we use thermal annealing of ZrO_2 overlayers on Pt in an ultra-high vacuum (UHV) system, where the background pressure during annealing was typically in the low 10^{-9} torr range. The predominant residual gases were the reducing gases, CO and H_2, whose partial pressure exceeds the partial pressure of the oxidizing gases H_2O and CO_2 by two-three orders of magnitude in a baked UHV system. Since we did not have deliberate control of the residual atmosphere, we cannot state definitively that from thermodynamic considerations Pt should reduce ZrO_2 on vacuum annealing, but the residual atmosphere in a UHV system is probably sufficiently reducing for the equilibrium to favor dissolution.

Zirconium carbide would be expected to form if metallic Zr were exposed to CO or hydrocarbons, but it is thermodynamically much less stable than the oxide. The carbide will, therefore, be reduced by Pt to form Pt-Zr alloys with vacuum annealing. The compounds reported in Table 1 are those actually expected to form in our experimental conditions of gas dosing or vacuum annealing. Other oxides of Pt and Zr exist, but are quite unstable. In principle, other types of compounds

are possible where both Pt-Zr and Zr-O bonds may be formed. At least one such compound (Zr_5Pt_2O) is reported in literature (4) but, unfortunately no thermodynamic data are available. From these considerations we can conclude that zirconium overlayers deposited on the platinum surface are metastable, and are expected to diffuse into the Pt bulk to form Zr-Pt alloys of low zirconium concentration upon vacuum annealing, or are expected to react readily upon dosing with oxygen, carbon monoxide or hydrocarbons.

3. EXPERIMENTAL

We used a UHV chamber equipped with quadrupole mass spectrometer and 3-grid LEED optics system. A single pass CMA with grazing incidence electron gun was used for Auger electron spectroscopy to detect the surface composition. AES peaks were recorded with a modulation amplitude of 2 V_{pp}, incidence angle about 15° and current density of about 3 μA/mm^2. The Pt sample was shaped as a disc about 1 mm thick. Both faces were cut and polished along the (100) face. The sample was attached to the manipulator by platinum wires spotwelded to the edges. It could be heated resistively up to about 1300 K. Temperatures were measured by a chromel-alumel thermocouple spotwelded to one of the faces.

The platinum surface as introduced was contaminated by sulphur, chlorine and carbon. A clean surface could be obtained by alternate cycles of ion bombardment and annealing. After this treatment the surface showed the $\begin{bmatrix} 14 & 1 \\ 1 & 5 \end{bmatrix}$ LEED pattern characteristic of the clean surface (5). Evidence of S and Ca. segregation to the surface was detectable only after protracted annealing at high temperature.

Metallic zirconium was evaporated by means of a commercial electron beam evaporator. The evaporator was located in a separately pumped chamber which could be isolated from the main chamber by a gate valve. Both faces of the Pt sample could be exposed to the zirconium flux. Pressure in the evaporation chamber was normally in the low 10^{-9} torr region and rose to the 10^{-8} torr range during evaporation. In the main chamber pressure was in the low 10^{-9} range during evaporation. Deposition rates varied as a function of the e^- beam current. Tests on glass substrates indicated rates up to 300Å/min at the evaporator-sample distance of 30 cm. One zirconium layer could be deposited in times that varied from 2 to 100 sec.

4. RESULTS

4.1 Zirconium Deposition and Growth on the Pt(100) Crystal Face

We used 99.99% purity metallic zirconium as starting material, with carbon and oxygen content nominally around 10 ppm by weight. However, it was not possible to obtain a deposited Zr layer completely free of oxygen and carbon. In Fig. 1, we show the AES spectrum of a Zr layer as deposited and of the same surface after exposure to oxygen. The oxygen peak for the "clean" surface is about 6% of the peak for the oxygen saturated surface. This result can be considered to represent the average initial purity of the Zr overlayers in this study. In general, the actual purity of the deposited film depended on the lifetime of the film in the vacuum chamber. Initially clean films showed detectable contamination from residual CO after a few minutes. Also, the purity of the film worsened detectably after several evaporations with the same Zr pellet in the evaporator.

Zirconium shows five main peaks in the AES spectrum (94, 116, 128, 147 and 174 eV). Tests performed by exposure to oxygen showed that the most intense peak (147 eV) (attributed to an $M_{4,5}N_{2,3}V$ transition in Ref. 6) is highly sensitive to oxygen adsorption. As shown in Fig. 1 the 147 eV peak is reduced in amplitude and splits into a doublet upon oxygen adsorption. Similar behavior has been reported (10) in the case of Zr on tungsten. However, since the peak overlaps significantly with the 150 eV Pt peak, quantitative analysis of peak shape variation was not possible for low zirconium coverages. The other Zr peaks showed a reduction in absolute amplitude upon oxygen uptake. However, their relative amplitude with respect to the platinum peaks remained approximately constant. The second most intense Zr peak (93 eV) overlaps with a Pt peak, therefore, the 116 eV peak ($M_5N_{2,3}N_{2,3}$) was considered the most suitable to provide a measure of the zirconium coverage on the surface.

Deposition tests were carried out by monitoring the variation of the Zr and Pt AES peaks after successive depositions of small amounts of zirconium on the surface. The process of successive depositions and AES recording was necessarily slow and substantial amounts of C and O contamination resulting from the reaction with residual CO were associated with Zr overlayers obtained in this way. A low degree of contamination could be obtained only when depositing at high rates and recording a small number of points. Results obtained in this way are shown in Fig. 2, together with growth curves obtained by deliberately exposing the deposited layer to oxygen in the 10^{-8} torr range between successive depositions (a procedure which reduced the carbon contamination).

In both cases the experimental points can be well fitted by successive straight lines, indicating a layer-by-layer growth mechanism. Both Pt and Zr peaks are reduced in absolute intensity upon oxidation. However, their ratio in correspondence to the monolayer break remains the same within the experimental error. The monolayer break corresponds to Zr(116 eV)/Pt(237 eV) AES ratio of about 1.8. CO adsorption did not appear to affect the growth of the overlayer, and the layer-by-layer mechanism was observed even in the case of highly carbon contaminated Zr surfaces.

4.2 LEED Results

Submonolayer amounts of Zr deposited at room temperature on the Pt(100) surface caused the $\begin{bmatrix} 14 & 1 \\ 1 & 5 \end{bmatrix}$ reconstructed surface structure to be replaced by a (1x1) structure which became progressively weaker and eventually disappeared as several Zr layers were deposited on the surface). Except for this change, no specific patterns attributable to zirconium were detected at room temperature (a (1 x 1) ordered Zr overlayer can be ruled out on the ground of the different atomic radius Zr = 1.60 Å, Pt = 1.39 Å). Patterns due to the overlayer could be obtained only by annealing the surface.

4.2.1 Zirconium Surface Structures

By annealing a surface covered with a zirconium multilayer around 900 K, we observed a reduction of the Zr AES signal attributable to Zr diffusion into the Pt bulk. At the same time ordering of the surface occurred and a c(2x2) surface structure was detectable by LEED (Fig. 3). The pattern was sharper at Zr (116 eV)/Pt(237 eV) AES ratios under 1.0, corresponding to a coverage smaller than a monolayer as determined from

the AES growth curves. This pattern can be attributed with certainty to zirconium. Sulphur is reported (7) to form a c(2x2) surface structure on the Pt(100) face, however, no sulphur was detectable by AES in our case.

As reported in the previous section, all the deposited zirconium films contained small amounts of oxygen. Also in the case of the c(2x2) structure some oxygen was detectable by AES, O(508 eV)/Zr(116 eV) ≈ 0.3. This amount is very small compared to the amount for the oxygen saturated surface, so that we can attribute the c(2x2) structure to clean zirconium. This conclusion is also supported by the observation that the c(2x2) surface structure disappeared upon exposure to CO. The c(2x2) structure weakened and disappeared upon heating and consequent further diffusion of the zirconium into the platinum bulk. The $\begin{bmatrix} 14 & 1 \\ 1 & 5 \end{bmatrix}$ structure was restored before total disappearance of the c(2x2) structure.

4.2.2 LEED Patterns of Oxidized Zr Layers on the Pt(100) Surface

Annealing a Zr overlayer exposed to either CO or O_2 at temperatures over 900 K caused partial diffusion of zirconium into the Pt bulk and the appearance of complex LEED patterns. AES observations showed that, after exposure to CO, and annealing, only oxygen was present on the surface, in addition to Zr.

The observed surface structures are summarized in Table 2. In most cases the patterns of the oxidized layer were of poor quality with a strong background. This indicates substantial disorder and, coupled with the complexity of some of the patterns, rendered their interpretation difficult. The first LEED pattern that was detectable after oxidation and annealing of a Zr overlayer is shown in Fig. 3.b. At first the pattern appeared very blurred for Zr(116 eV)/Pt(236 eV) ratios

around 2.6 (higher than a monolayer). This pattern consists of two well defined rings of spots; the inner one is formed by a total of 24 spots the outer one by 16 spots. Other weaker spots appear in the picture of Fig. 3; these are attributed to other structures and/or to double diffraction. The two rings always appear together and have to be interpreted as part of the same structure. The interpretation of the LEED pattern is shown in Fig. 5, and the unit cell is reported in Table 1. The unit cell dimensions appear to be slightly variable depending on zirconium coverage, as one would expect for an incommensurate structure. There are two different phases, which have a very similar rhombic unit cell, almost exactly superimposable by a rotation of 45°. Each phase shows two equivalent domains rotated 90° with respect to each other. Both phases have rhombic unit cells incommensurate with respect to the substrate unit cell. Simple epitaxial relationships with the substrate plane are, however, present. The two phases usually appeared with the same spot intensity. The $\begin{bmatrix} 1.08 & 0 \\ 0.27 & 1 \end{bmatrix}$ appeared, however, to be slightly more stable, since its pattern tends to persist for a longer time upon annealing and diffusion of Zr into the Pt bulk. Annealing a surface showing the rhombic pattern led to the appearance of further spots corresponding to complex patterns. These patterns were generally too complex and of too poor quality for an interpretation, although at least some of the spots could be regarded as the result of double diffraction from the rhombic structures. Further annealing at temperatures where zirconium diffuses into the Pt bulk led to the weakening and gradual disappearance of the rhombic structure. New LEED patterns appeared depending on the degree of oxidation of the zirconium.

If very pure deposited zirconium was exposed only to CO and annealed under conditions which caused the disappearance of the carbon from the surface, the LEED pattern which replaced the rhombic structure was for the $\begin{bmatrix} 7 & 0 \\ 0 & 4/3 \end{bmatrix}$ structure. If the Zr layer was exposed to oxygen at pressures in the 10^{-7} torr range or lower, or an oxygen contaminated Zr pellet was used in the evaporation, the $\begin{bmatrix} 2 & 1 \\ \bar{1} & 1 \end{bmatrix}$ structure was observed to exist at the same time as the $\begin{bmatrix} 7 & 0 \\ 0 & 4/3 \end{bmatrix}$. If the oxygen exposure was carried out at pressures in the 10^{-6} range or higher, only the $\begin{bmatrix} 2 & 1 \\ \bar{1} & 1 \end{bmatrix}$ was observed. Usually the $\begin{bmatrix} 7 & 0 \\ 0 & 4/3 \end{bmatrix}$ pattern appeared as streaks, where it was very difficult to detect individual spots (Fig. 3d). Therefore, the periodicity along the short axis of the reciprocal unit cell is uncertain. On the other hand, the 4/3 periodicity along the long axis is well established from observations of multiple order features. The $\begin{bmatrix} 7 & 0 \\ 0 & 4/3 \end{bmatrix}$ structure appeared for a Zr (116eV)/Pt(237eV) ratio under about 1.5 and traces of the same structure were detectable for ratios around 0.2. The unit cell for this structure is shown in Fig. 4. The O(503 eV)/Zr(116 eV) AES ratio associated with the $\begin{bmatrix} 7 & 0 \\ 0 & 4/3 \end{bmatrix}$ structure was never higher than about 1.8, and was usually lower depending on the condition of annealing. The variation of the oxygen content appeared to affect the periodicity along the short axis of the reciprocal unit cell. The $\begin{bmatrix} 7 & 0 \\ 0 & 4/3 \end{bmatrix}$ was apparently associated with the Pt reconstruction since it was never detectable in conjunction with a Pt(1 x 1) pattern. In Fig. 3d, only one of the two possible domains has formed. However, in some cases both domains (rotated 90°) were observed in the same pattern, depending on the conditions of preparation of the surface. In other cases, traces of a similar pattern were detected for very low Zr coverages, Zr(116 eV)/Pt(237 eV) = 0.2-0.3, in correspondence with little

or no oxygen detectable in the AES spectrum. Due to the faintness of the pattern, accurate observations are not possible. However, it appears that this structure can be described as a $\begin{bmatrix} 5 & 0 \\ 0 & 4/3 \end{bmatrix}$, with the (4/5, 3/4) spots especially intense. The periodicity along the short axis of the reciprocal unit cell is, in this case, the same as the Pt $\begin{bmatrix} 14 & 1 \\ 1 & 5 \end{bmatrix}$ reconstruction.

The $\begin{bmatrix} 2 & 1 \\ 1 & 1 \end{bmatrix}$ phase could be obtained after exposure to oxygen and partial diffusion into the Pt bulk of a Zr multilayer. In contrast to the other patterns for oxidized zirconium, the $\begin{bmatrix} 2 & 1 \\ 1 & 1 \end{bmatrix}$ appeared very well ordered with sharp spots. For low coverages, this pattern was usually associated with the Pt $\begin{bmatrix} 14 & 1 \\ 1 & 5 \end{bmatrix}$ reconstruction. The reciprocal unit cell is shown in Fig. 4b. The O(508eV)/Zr(116 eV) AES ratio associated with the $\begin{bmatrix} 2 & 1 \\ 1 & 1 \end{bmatrix}$ structure was variable, depending apparently on the presence on the surface of disordered Zr phases with different (usually lower) degree of oxidation. The ratio also depended on the presence of oxygen associated with platinum. The O/Zr ratios observed range from 2.2 to about 3.0 for a "pure" $\begin{bmatrix} 2 & 1 \\ 1 & 1 \end{bmatrix}$ pattern after strong oxidation. The $\begin{bmatrix} 2 & 1 \\ 1 & 1 \end{bmatrix}$ structure could also be obtained exposing a surface showing the rhombic patterns to 10^{-4} torr of O_2 at room temperature. (Lower pressures were sufficient at higher temperatures.) This caused the rhombic pattern to disappear, leaving only the Pt(1 x 1) pattern associated with a strong background. Subsequent flashing over 900 K produced the $\begin{bmatrix} 2 & 1 \\ 1 & 1 \end{bmatrix}$ structure without detectable diffusion of Zr in the Pt bulk. If the $\begin{bmatrix} 2 & 1 \\ 1 & 1 \end{bmatrix}$ itself was exposed to O_2 at 10^{-4} torr we observed the reversible transformation $\begin{bmatrix} 2 & 1 \\ 1 & 1 \end{bmatrix} \rightleftarrows$ (1 x 1) upon annealing. The process could be repeated several times, as illustrated in Fig. 5.

4.3 Zirconium Bulk Diffusion and Surface Segregation

We found that metallic zirconium deposited on the Pt(100) face diffuses into the Pt bulk at temperatures around 500 K. Higher temperatures caused more rapid diffusion. This process is illustrated in Fig. 6 for different temperatures. Besides temperature, two factors affect the diffusion rate: one is the degree of oxidation of the Zr overlayer, the other the presence of zirconium from previous diffusion into the Pt bulk.

If the zirconium layer was partially oxidized, we observed a considerable enrichment in oxygen of the overlayer during the diffusion process. Highly oxidized zirconium diffused less rapidly than metallic zirconium. However, diffusion also took place in this case presumably involving decomposition of the Zr oxide. Oxidized zirconium disappeared from the surface upon annealing around 1200 K. Total disappearance of the zirconium from the surface was obtainable by annealing only if the Pt bulk was free of zirconium. After several deposition/bulk diffusion cycles we observed a residual Zr AES signal which could not be eliminated by annealing. Depth profiling of the surface revealed the presence of zirconium in the Pt bulk. During depth profiling the value of the Zr(116 eV)/Pt(237 eV) AES ratio was around 0.1-0.2. This value remained approximately constant after removing an estimated 10^3 Å of surface. Only extraction of the sample from the vacuum chamber and removal of an approximate 0.1 mm of surface by chemical etching could produce the complete disappearance of the AES Zr signal.

The presence of zirconium in the Pt bulk caused segregation phenomena. Annealing the surface in ultra high vacuum after ion bombardment produced a reduction of the Zr AES signal, corresponding to platinum

segregation to the surface. This process is reversible since zirconium resegregates to the surface upon cooling. Equilibrium conditions are reached in a few minutes at temperatures over 900 K. It is important to note that only oxygen free zirconium segregates to the surface in these conditions even if most of the previously diffused zirconium was in the form of an oxide. As a result, independent from the initial coverage and degree of oxidation, it was possible to obtain a completely clean zirconium layer by annealing the surface at 1200 K for a time sufficient to cause the complete dissolution of the Zr oxide present on the surface. Subsequent cooling caused the segregation of small amounts of zirconium with Zr(116 eV)/Pt(237 eV) $\simeq$ 0.2.*

Oxidized zirconium could be segregated at the surface of the Pt sample by annealing over 900 K in the presence of oxygen at pressures in the 10^{-6} range or higher. Regardless of temperature and oxygen pressure, the amount of zirconium segregation was always below a monolayer. The overlayer was highly oxidized, with O(508 eV)/Zr(116 eV) AES ratios around 3.0. The LEED pattern observed was for the $\begin{bmatrix} 2 & 1 \\ 1 & 1 \end{bmatrix}$ structure.

4.4 Reaction of the Zr Overlayer with O_2, CO and Hydrocarbons

4.4.1. Reaction with O_2

Zr deposited on Pt was found to be highly reactive towards oxygen. This behavior is similar to that of the pure metal (8,14). In Fig. 7 we show the oxygen peak-to-peak height versus time for a monolayer and a multilayer of zirconium deposited at room temperature for oxygen exposure at 1 x 10^{-8} torr. The initial stage of oxidation is the same in both

*No oxygen was detectable by AES after this treatment.

cases and the curve can be interpreted as a straight line, indicating a constant sticking coefficient. In the case of the Zr monolayer, the oxygen uptake reaches a plateau, which, however, continues growing very slowly with time. The oxygen uptake is more rapid for the multilayer, but eventually both curves level off after several hours of exposure, showing approximately the same oxygen signal.

In the case of a monolayer, the O(508 eV)/Zr(116 eV) AES ratio equals 1.8 at the beginning of the plateau. In the case of multilayers, the AES ratio had a lower value which in general depended on the layer thickness. This indicated that under these conditions of deposition the initial oxidation involved only the topmost layer.

From the linear part of the curve in Fig. 13, we can obtain an estimate of the initial sticking coefficient for oxygen. Assuming that the Zr concentration is 1.1×10^{19} atoms/m^2 (as in the [0001] plane of the pure metal), and assuming a one-to-one stoichiometry, we obtain a value equal to about 0.9, which can be assumed to be unity within the experimental error. This value is in good agreement with the results reported by Foord, et al. (8).

Thermal treatment of the deposited Zr layer affected the oxidation rate. Surfaces which were annealed at temperatures where substantial zirconium diffusion into the Pt bulk took place reacted with oxygen at a slower rate in comparison to not-annealed surfaces. This effect was especially pronounced in the case of the surface obtained (as described in 3.3) by strong annealing and successive resegregation of very clean zirconium. As shown in Fig. 8, under these conditions, zirconium does not detectably uptake oxygen for pressures up to 1×10^{-6} torr, in

contrast to the not-annealed layer which reacts already at 10^{-8} torr. However, the result of oxidation at high pressure and temperature was about the same regardless of the pretreatment of the surface. The highest value of the O(503 eV)/Zr(116 eV) AES ratio obtainable by oxidation was about 3.0 at the highest pressure compatible with our vacuum system ($\approx 10^{-4}$ torr). We also examined the surface of a sample after zirconium deposition, annealing and exposure to air at atmospheric pressure using spatially resolved scanning AES. The value of the O/Zr AES ratio appeared to be the same ($\approx$3.0), and the surface was found to be homogeneous in zirconium and oxygen with no traces of extensive phase separation.

4.4.2. Reaction with CO

We obtained growth curves for the O(503 eV) AES peak, following exposure of a zirconium overlayer to a constant pressure of CO in the 10^{-8} torr. In this case, the curve reaches a plateau after exposure over about 1 Langmuir. The saturation O(503 eV)/Zr(116 eV) AES ratio was about 1.1, and the O(268 eV)/Zr(116 eV) about 0.9 for a monolayer. The shape of the AES carbon peak was clearly indicative of the carbide state (Fig. 9) and since no significant CO desorption was detected after exposure to CO of a surface totally covered with Zr, it can be concluded that CO adsorption was dissociative, resulting in the formation of zirconium carbide and oxide on the surface.

In contrast with the results obtained with oxygen, no further growth of the oxygen or carbon peak could be obtained for exposures at longer time or at higher pressures of CO. Annealing a Zr layer previously saturated with CO at temperatures over 900 K produced a gradual reduction of the relative intensity of the carbon AES peak and an increase in the

relative intensity of the oxygen peak (Fig. 9). At this temperature AES data showed partial dissolution of the Zr layer into the Pt bulk. The final result of protracted annealing was a completely carbon free surface, still containing zirconium and oxygen. Such a surface had an O(503 eV)/Zr(116 eV) AES ratio equal to about 1.9 or less and showed the $\begin{bmatrix} 7 & 0 \\ 0 & 4/3 \end{bmatrix}$ LEED pattern. The mechanism of carbon elimination is not completely clear. When carbon and oxygen were present on the surface, CO and CO_2 were detected by mass spectrometry to desorb from the sample with annealing to over 900 K, but the O/Zr AES ratio was observed to increase. We conclude, therefore, that part of the carbon was eliminated by diffusion into the platinum bulk. Oxidized zirconium layers did not detectably adsorb CO. Reversible CO adsorption was detected only when free Pt surface was available.

Annealed zirconium overlayers were observed to have significantly reduced reactivity with respect to CO, e.g. no dissociative CO adsorption was observed (for pressures up to about 1×10^{-8} torr) for an annealed surface with the Zr(116 eV)/Pt(237 eV)= 0.2. The reduced reactivity of the annealed surfaces for carbon monoxide is similar to the effect observed for the reaction with oxygen described in the prior section.

5. DISCUSSION

5.1 Clean Zr Deposition and Structure on the Pt(100) Crystal Face

Metal deposition on single crystal metal surfaces is a well studied subject (9). It is known that the growth mechanism is controlled by the relative strength of the metal-substrate bond, as compared to the strength of the bond in the pure metal. In the case of zirconium and platinum, the metal-substrate interaction involves a strong intermetallic bond (1). Therefore, one would predict that the energy of the system would be minimized if the zirconium layer spreads evenly on the Pt surface. Indeed, a layer-by-layer growth mechanism has been observed. It is interesting to note that the same growth mechanism is maintained even if the surface zirconium is slightly oxidized or has reacted with CO. It appears, therefore, that the carburization and oxidation in these conditions does not involve the breaking of the Pt-Zr bond. Presumably, the formation of the fully oxidized compound (ZrO_2) on the surface would instead involve the formation of 3D crystallites.

Compared to other metal/metal systems one difference in the Zr/Pt(100) system is the lack of ordering of the overlayer after deposited at room temperature. The only effect observed, the disappearance of the Pt $\begin{bmatrix} 14 & 1 \\ 1 & 5 \end{bmatrix}$ reconstruction in favor of the simple Pt(1x1), cannot be attributed to the formation of an ordered (1x1) Zr overlayer (it would require a 13% contraction of the Zr atomic radius). Rather, small amounts of zirconium on the surface have apparently the effect of destabilizing the $\begin{bmatrix} 14 & 1 \\ 1 & 5 \end{bmatrix}$, an effect which has been observed in the case of other adsorbates such as CO. The absence of LEED patterns formed at room temperature is not in contrast with the observed growth mechanism. For a "layer-by-layer"

growth mechanism to occur, the mobility of zirconium on zirconium must be large. However, if the mobility of zirconium on platinum is very low, many small 2D crystallites will form during deposition. The low Zr mobility will prevent coalescing into larger crystallites and the resulting surface will be formed of 2D island which are too small and disordered to produce a detectable LEED pattern.

The same kind of behavior has been observed for zirconium growth on the W(100) surface (6, 10,11). Also, in this case, the observed growth mechanism was layer-by-layer, but it was necessary to anneal or to deposit at high temperature in order to obtain LEED patterns from the overlayer. The observed low mobility of the deposited Zr on both Pt and W can, in principle, be explained as due either to strong Pt-Zr interaction or to the presence of oxygen in the zirconium layer. To make a definitive distinction, it would be necessary to deposit clean zirconium. Unfortunately, this was unattainable in our apparatus. Substantial oxygen contamination was presumably present in the work of Hill, et al.,(10) on the Zr/W system and traces of oxygen are reported in the works of Davis (6) and Danielson and Swanson (11) on the Zr/W system. The only "clean" Zr pattern detected, the c (2x2) appears to correspond to a coverage smaller than a monolayer, according to the AES calibration reported in Fig. 2. We remark, however, that since this pattern could be observed only after partial diffusion of the zirconium into the Pt bulk, the surface structure could be substantially modified with formation of a mixed Pt-Zr overlayer (surface alloy). In this event, the AES calibration obtained at room temperature would not be applicable any more.

5.2 Zr Diffusion/Segregation

Taking into account the highly negative free energy of solution for zirconium into platinum (12), it is not surprising that zirconium has been found to diffuse into the platinum bulk at relatively low temperatures (diffusion is detectable at temperatures as low as 800 K). A similar behavior has been found for the Zr/W(100) system (6,11). Thermodynamic considerations also indicate that oxidized zirconium should decompose and Zr diffuse into the Pt bulk by annealing in vacuum. We found this to occur at higher temperatures than those required for clean Zr dissolution. This observation appears to be easily explained, since the diffusion presumably requires breaking the very stable Zr-O bond. An alternative mechanism involves the diffusion into the Pt bulk of the zirconium as an oxide, but this would be in conflict with the observed segregation of pure zirconium from the Pt bulk, which suggests that the Zr in the bulk is in the form of pure metal. In the Zr/W(100) system, oxidized zirconium was found to diffuse in the W bulk more easily than pure zirconium (6). According to Davis (6), this could be explained by taking into account the fact that Zr bound to oxygen is ionized, and therefore of smaller diameter, which should ease its diffusion under the surface. Since the Pt-Zr bond is stronger than the W-Zr bond, even if the same factors involving the atomic diameter are present, the pure Zr diffusion may still be favored in our case.

After the bulk diffusion into platinum of a substantial amount of zirconium our sample could be regarded as a low Zr concentration Pt/Zr alloy. This system should exhibit surface segregation phenomena and our data indicate a complex Zr behavior in this respect. The formation of

oxidized Zr layer on the surface by annealing in the presence of oxygen is in keeping with the energetic gain resulting from the formation of the zirconium oxide predicted by thermodynamics. The segregation phenomena observed upon annealing in vacuum are not as easily understood. Our results indicate that at high temperature the surface is enriched in platinum with respect to the bulk. This can be explained qualitatively in the framework of the broken bond approximation (2). The difference in binding energy of the pure metals is small, since the Zr heat of vaporization (145 kcal/mol) is slightly higher than that of Pt (135 kcal/mol) (16). Since the Pt-Zr bond is stronger than either the Pt-Pt or Zr-Zr bond, the lowest free energy is obtained by maximizing the number of those bonds by removing the minority compounds (Zr) from the surface.

5.3 Zr Interaction with Gases

The interaction of the deposited Zr with oxygen is of particular interest in view of the catalytic properties of the Pt_3Zr alloy for oxygen reduction (3). As discussed before thermodynamic considerations indicate that the formation of ZrO_2 is favored in the presence of oxygen. Therefore, one would expect zirconium deposited on platinum to oxidize easily, and this is the observed behavior for overlayers (monolayers or multilayers) deposited at room temperature. The kinetics of oxygen adsorption on the surface show little dependence on the overlayer thickness (Fig. 13), however, they are markedly affected by the previous thermal treatment, as shown in Fig. 4. In particular, the surface resulting from strong annealing and successive surface segregation of a small amount of clean zirconium appears to be relatively unreactive both with respect to CO and O_2.

This result can be explained in two ways.

1) a pure Pt overlayer which prevents the contact of the Zr atoms with the gas molecules (steric effect);

2) Change of the zirconium properties due to the Zr electronic interaction with the substrate (ligand effect).

Both factors could be present in an intermediate situation in which zirconium and platinum form a surface alloy where zirconium atoms are only partially exposed in the surface and also show a ligand effect. The Engel-Brewer interpretation of the intermetallic bond (1) predicts a strong change in the electronic and chemical properties of the atoms due to strong intermetallic bonding. However, the fact that annealing is necessary to observe this effect is an argument against such an explanation: a monolayer which has not been annealed reacts with CO and O_2 just as pure zirconium despite the fact that a Pt-Zr bond is present. Annealing may increase the number of Pt-Zr bonds, by the formation of surface alloys and therefore increase the effect. However, it is difficult to explain in just these terms the drastic change in reactivity observed. We therefore conclude that a surface composition effect due to the formation of surface containing no Zr <u>on</u> the surface is a more likely explanation.

AES observations alone are not sufficient to establish the O/Zr atomic ratio for the oxidized Zr overlayer. However, by analogy with the results for pure zirconium (8,14), we may assume that in our case stoichiometric ZrO_2 is not formed by exposure to oxygen at low pressure at room temperature. Also, in the case of the ordered oxidized structures obtained by annealing (rhombic, $\begin{bmatrix} 7 & 0 \\ 0 & 4/3 \end{bmatrix}$, $\begin{bmatrix} 2 & 1 \\ 1 & 1 \end{bmatrix}$), the exact stoichiometry cannot be determined. However, the fact that these phases exhibit a well defined

epitaxial relationship with the substrate implies the formation of a Zr-Pt bond. Such a bond would presumably block complete oxidation of the zirconium atoms, so that the observed phases represent lower oxidation states of zirconium, stabilized by the presence of platinum.

The rhombic phases (see Table 2) can be regarded as deriving from the Zr(0001) hexagonal plane by enlarging the angle and shortening the Zr-Zr distance. If we assume one Zr atom per unit cell and all atoms in the same plane, the observed Zr-Zr distance of 3.0 Å represents a 6% contraction with respect to the pure metal, some contraction should be expected since Zr is bound to oxygen and therefore, partly ionized (Zr^0 radius is 1.60 Å, Zr^{4+} is 0.8 Å). No information can be obtained on the position of the oxygen atom (or atoms) in the unit cell from examination of the LEED patterns without intensity analysis. The other two structures observed, $\begin{bmatrix} 2 & 1 \\ \bar{1} & 1 \end{bmatrix}$ and $\begin{bmatrix} 7 & 0 \\ 0 & 4/3 \end{bmatrix}$, involve large unit cells which may contain more than one Zr atom. Little information can be obtained from LEED patterns about the actual surface structure. However, considering the high stability of the Pt-Zr bond and the necessity of strong annealing to obtain the patterns, it is likely that both structures involve a substantial rearrangement of the Pt surface. Of particular interest is the reversible transformation $\begin{bmatrix} 2 & 1 \\ \bar{1} & 1 \end{bmatrix} \rightleftharpoons (1 \times 1)$ which occurs with high exposure to oxygen and successive annealing.

In this transformation, oxygen was desorbed from the surface when passing from the (1 x 1) to the $\begin{bmatrix} 2 & 1 \\ \bar{1} & 1 \end{bmatrix}$. This oxygen is likely to be associated with platinum since: i.) it desorbs at the same temperature as from a pure Pt(100) surface; ii.) it reacts with CO so that no oxygen desorption is detectable after a sufficiently high exposure to CO. The

Table 2. Surface Structures for the Pt(100)/Zr/O System.

Structure	Unit Cell Dimen. Å	Angle of Unit Vectors	Unit cell Area $Å^2$	Zr(116eV)/Pt(237eV) AES Ratio	O(508eV)/Zr(116eV) AES Ratio	Comments
Pt(100) 1x1	2.78,2.78	90°	7.7	-	-	Substrate
Pt(100) c(2x2)-Zr	3.92,3.92	90°	15.46	0.4 - 0.7	≃0.3	"Clean" Zr
$\begin{bmatrix} 1.08 & 0 \\ 0.27 & 1 \end{bmatrix}$	3.00,2.98	74.9°	8.3	1.4 - 2.6	≃2.0	Rhombic
$\begin{bmatrix} 0.77 & 0.77 \\ \overline{0.57} & 0.92 \end{bmatrix}$	3.02,3.01	76.8°	8.8	1.4 - 2.6	≃2.0	Rhombic
$\begin{bmatrix} 2 & 1 \\ \overline{1} & 1 \end{bmatrix}$	6.22,3.92	108.4°	23.1	0.2 - 1.9	2.5-3.0	Results from exposure to O_2
$\begin{bmatrix} 7 & 0 \\ 0 & 4/3 \end{bmatrix}$	19.5,3.7	90°	72.1	0.2 - 1.0	≃1.8	Results from exposure to CO

"clean-off" reaction is characteristic of Pt (17), and we never detected a reduction of the oxygen signal when the $\begin{bmatrix} 2 & 1 \\ \bar{1} & 1 \end{bmatrix}$ surface was exposed to CO.

On the basis of these considerations, it seems reasonable to consider the (100)-(1x1) structure as islands of ZrO_2 on top of the (100)-(1x1) Pt surface. These islands are out of registry with each other, and with the substrate and appear only as the high background in the (1x1) LEED pattern. The 900 K annealing partially reduces these ZrO_2 islands, and dissolves zirconium <u>into</u> the surface, together with some oxygen ligands. The Zr^{4+} ion is much smaller than the metallic Zr atom, which is much larger than the Pt atom. The Zr^{4+} ion can penetrate the Pt surface more easily than Zr^0 as an interstitial, and can do so while retaining an oxygen ligand at the surface. The $\begin{bmatrix} 2 & 1 \\ \bar{1} & 1 \end{bmatrix}$ structure is, therefore, suggested to be a Pt Zr_xO_y metastable surface phase, which can be fully reduced to form a Pt-Zr alloy bulk phase at higher temperature (1200 K) and can be oxidized to separate ZrO_2 and Pt bulk (or dispersed) phases.

6. CONCLUSION

Zr overlayers of various thickness have been grown on the Pt(100) surface by thermal evaporation of the metal. A layer-by-layer growth mechanism was observed, even when zirconium was oxidized at low pressure between successive depositions. Zirconium layers deposited at room temperature were highly reactive towards oxygen, carbon monoxide and hydrocarbons. Several metastable ordered structures were observed by LEED when oxidized overlayers were thermally annealed in UHV. Annealing at 900 K resulted in the diffusion of metallic zirconium into the platinum bulk, but higher temperatures were necessary to obtain reduction and dissolution of oxidized overlayers. The ultimate result of sufficiently

protracted annealing was the complete disappearance of zirconium from the surface, regardless of the initial degree of oxidation. Solid state diffusion of metallic zirconium in Pt appeared to be the rate determining factor for the dissolution of the overlayer. Annealed surfaces were unstable with respect to oxygen. Oxygen dosing at room temperature caused resegregation of zirconium to the surface, and formation of an ordered Pt Zr_xO_y surface phase. This phase was stable in oxygen at temperatures between 25 and 300°C. Dosing at 300°C and higher caused precipitation of ZrO_2 islands on top of the Pt(100)-(1x1) surface.

ACKNOWLEDGMENTS

PNR acknowledges the support of the Assistant Secretary for Fossil Energy, Office of Fuel Cells, Advanced Concepts Division and GAS acknowledges the support of the Director, Office of Energy Research, Office of Basic Energy Sciences, Materials Science Division of the U.S. Department of Energy under Contract #DE-AC03-76SF00098. The authors thank Drs. M. Jazzar and M. Salmeron for their advice and comments.

REFERENCES

1. L. Brewer, "Viewpoints of Stability of Metallic Structures," in Phase Stability in Metals and Alloys, edited by P. Rudman, J. Stringer and R. I. Jaffee, MacGraw-Hill, NY 1967, p. 39.
2. W. M. H. Sachtler and N. A. Van Santen, Application of Surface Science 3 (1979), 121-144.
3. P. N. Ross, EPRI Final Report EM-1553, Project 1200-5, Sept. 1980.
4. M. V. Nevitt, J. W. Downey and R. A. Morris, AIME Trans. 218 (1960) 1019.
5. S. B. Hagstrom, H. B. Lyon and G. A. Somorjai, Phys. Rev. Lett. 15 (1965) 491.
6. P. R. Davis, Surf. Sci. 91 (1980) 385.
7. Y. Berthier, M. Perdereau and J. Oudar, Surf. Sci. 36 (1973) 223.
8. J. S. Foord, P. J. Goddard and R. M. Lambert, Surf. Sci. 94 (1980) 339.
9. J. P. Biberian and G. A. Somorjai, J. Vac. Sci. Technol. 16 (9) (1979) 2073.
10. G. E. Hill, I. Marklund and L. W. Swanson, Surf. Sci. 24 (1971) 435.
11. L. R. Danielson and L. W. Swanson, Surf. Sci. 88 (1979) 14.
12. P. J. Meschter and W. L. Worrell, Metallurgical Transactions 8A (1977) 503.
13. JANAF Thermochemical Tables, Second Edition, NSRDS-NBS 37, 1971.
14. E. Fromm and O. Mayer, Surf. Sci. 74 (1978) 259.
15. L. Brewer and P. R. Wengert, Metallurgical Transactions 4 (1973) 83.

16. O. Kubaschewski and C. B. Alcock, Metallurgical Thermochemistry, Pergamon Press, 1979.

17. D. Monroe and R. Merrill, J. Catal., 65, 461 (1980).

FIGURE CAPTIONS

1) AES spectrum of the Pt(100) surface after deposition of about 2 Zr layers- curve 1) immediately after deposition; curve 2) after exposure to O_2 P = $1x10^{-6}$ torr x 3 mins.

2) Growth curves for successive depositions of zirconium on the Pt(100) surface. O, ●: Zr(116); Δ, ▲ Pt(237). Open symbols for as-deposited Zr. Closed symbols for successive deposition with 0.2L oxygen doses.

3) Observed LEED patterns - a) Pt(100)-c(2x2)- Zr, E = 99 eV; b) rhombic pattern, E = 74 eV; c) $\begin{bmatrix} 2 & 1 \\ 1 & 1 \end{bmatrix}$ E = 46 eV; d) $\begin{bmatrix} 7 & 0 \\ 0 & 4/3 \end{bmatrix}$, E = 54 eV.

4) Interpretations of the LEED patterns. a) Rhombic; b) $\begin{bmatrix} 2 & 1 \\ 1 & 1 \end{bmatrix}$; c) $\begin{bmatrix} 7 & 0 \\ 0 & 4/3 \end{bmatrix}$. Open circles : Pt(100) spots.

5) Schematic sequence of LEED patterns observed on the Pt(100) surface upon zirconium deposition, annealing and oxidation.

6) Zr(116 eV)/Pt(237 eV) AES ratio for successive annealings at increasing temperature. Initial O(503 eV)/Z_r(116 eV) AES ratio = 0.3, final (after annealing 1200 K) = 2.5.

7) Oxygen adsorption on an initially clean Zr monolayer (full circles) and multilayer (open circles).

8) Effect of previous annealing on reactivity.

   Δ: surface after Zr deposition at room temperature

   O: surface obtained by annealing at 1200 K and successive resegregation of clean zirconium

9) Progressive disappearance of the carbon peak for a zirconium multilayer deposited on Pt(100) and exposed to CO at room temperature. From top to bottom each AES spectrum corresponds to successive annealings at 973 K.

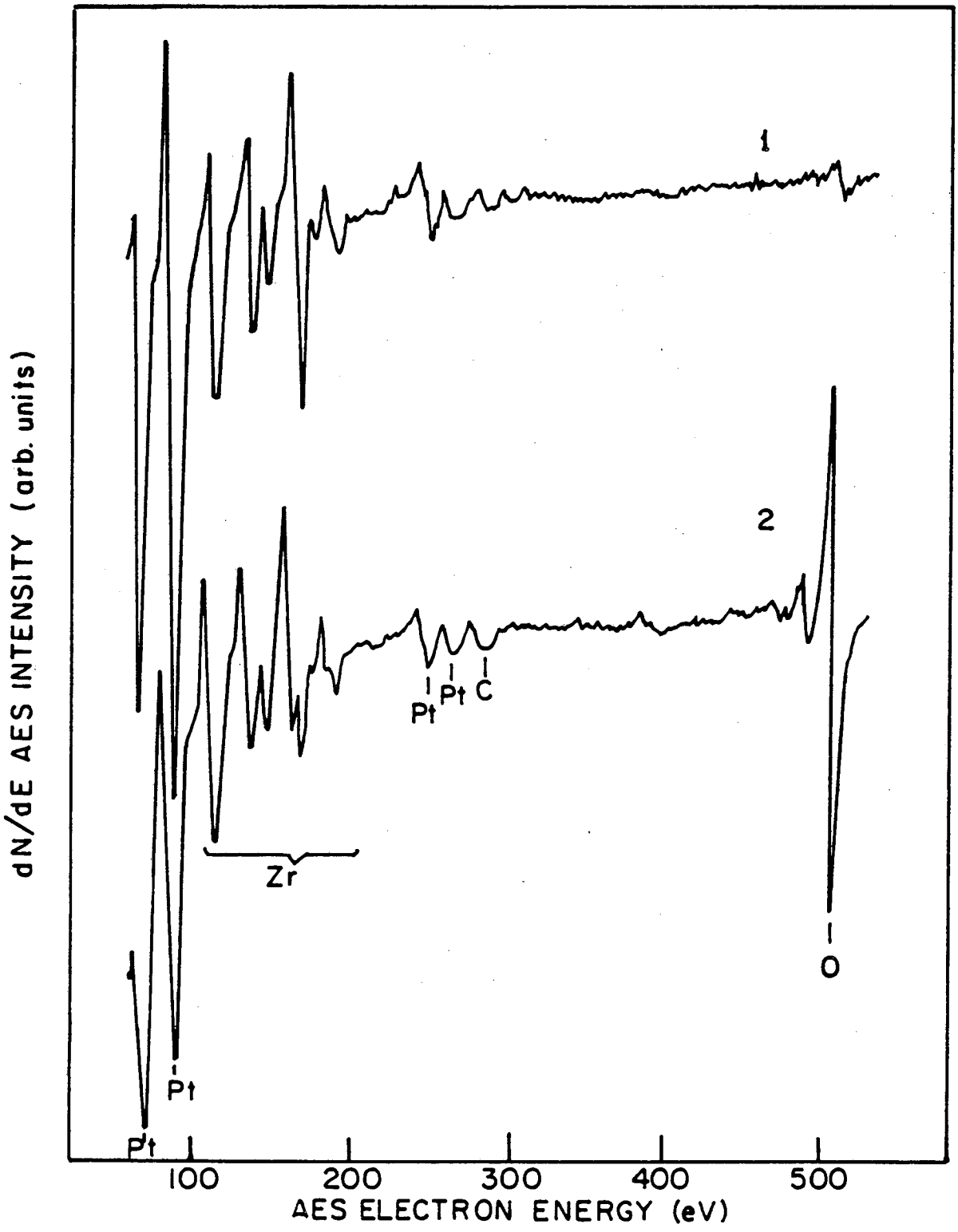

XBL 828-6410

Fig. 1

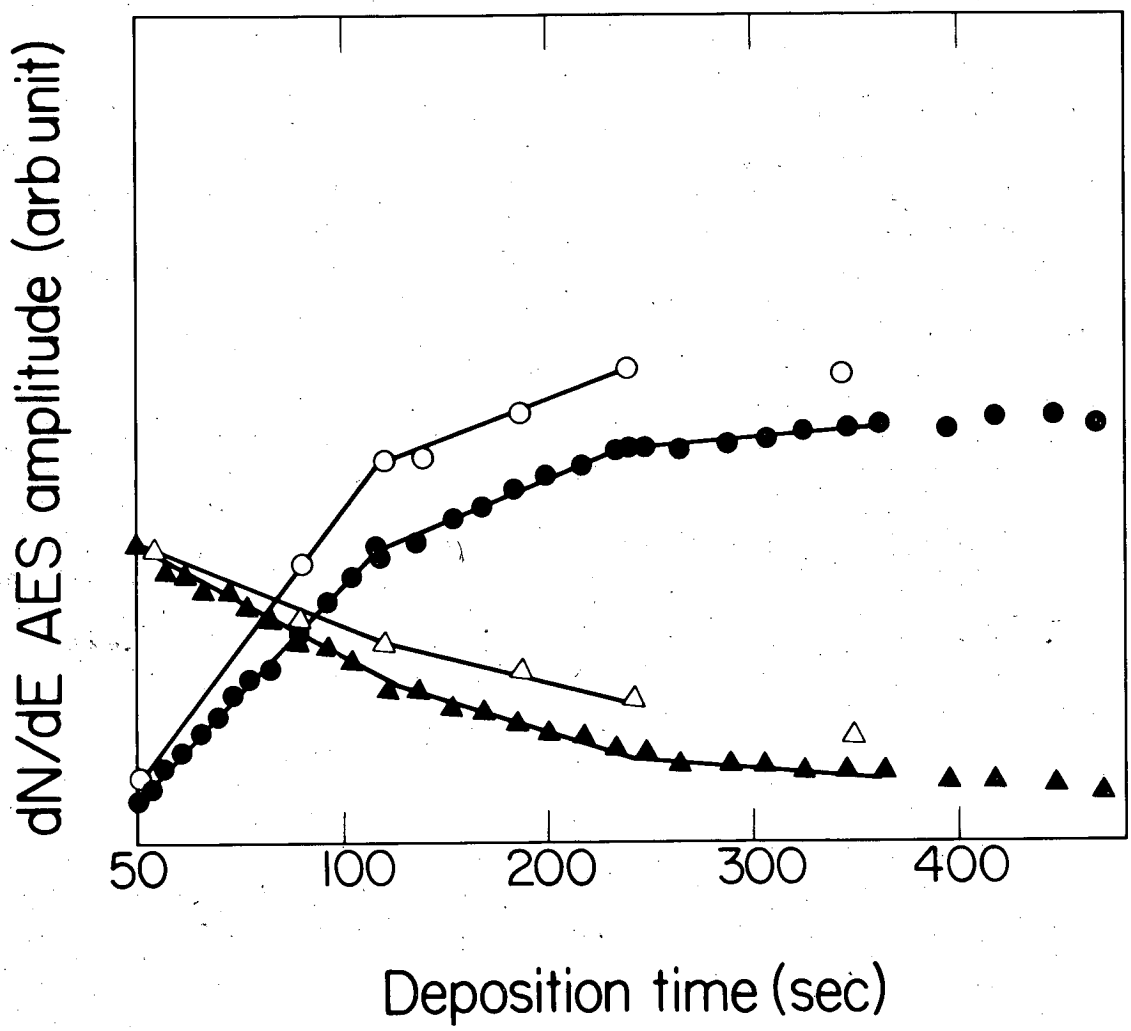

XBL-829-4563

Fig. 2

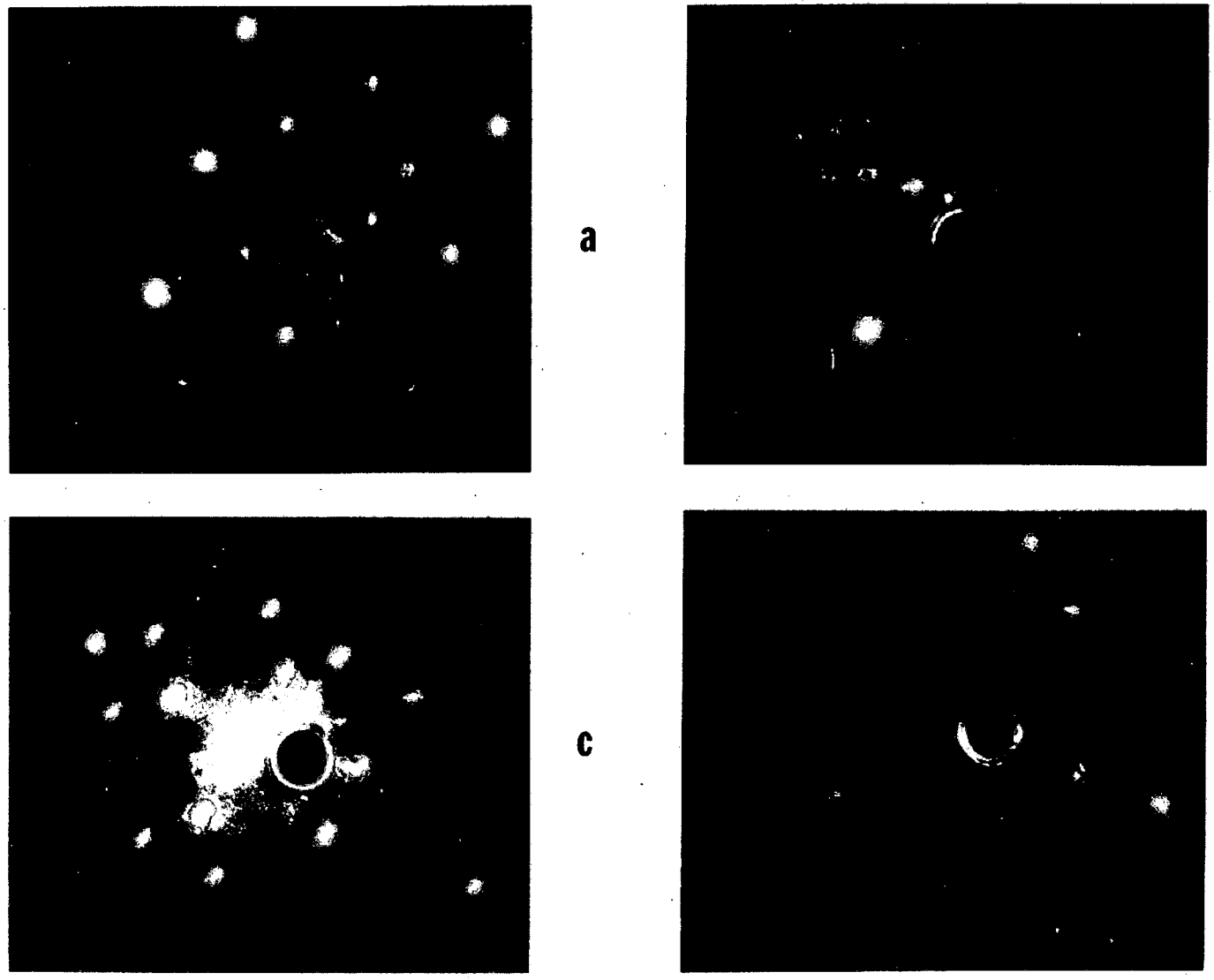

XBB820-9936

Fig. 3

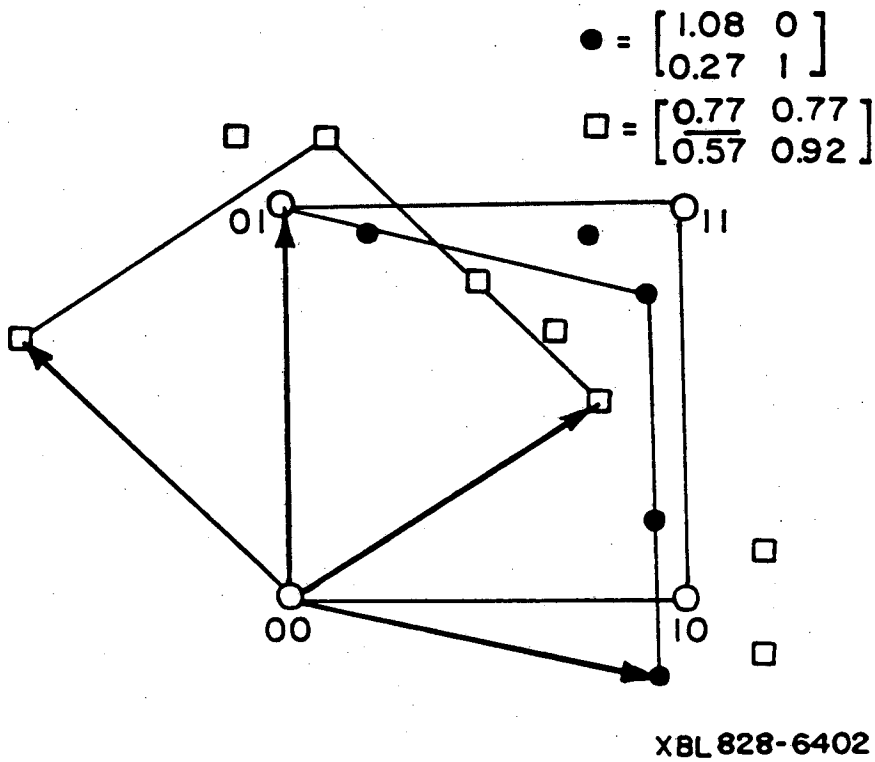

Fig. 4a

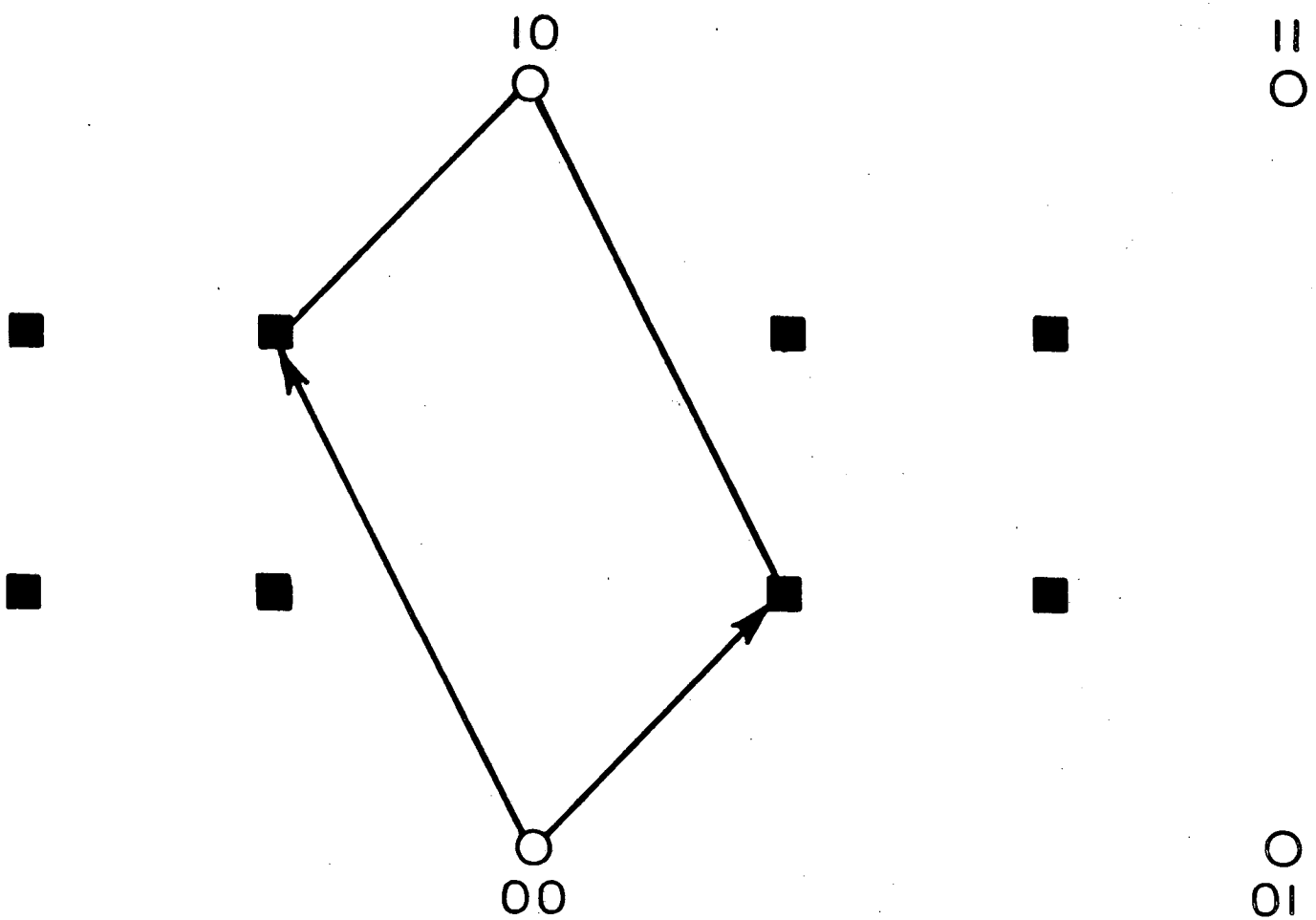

XBL 828-6413

Fig. 4b

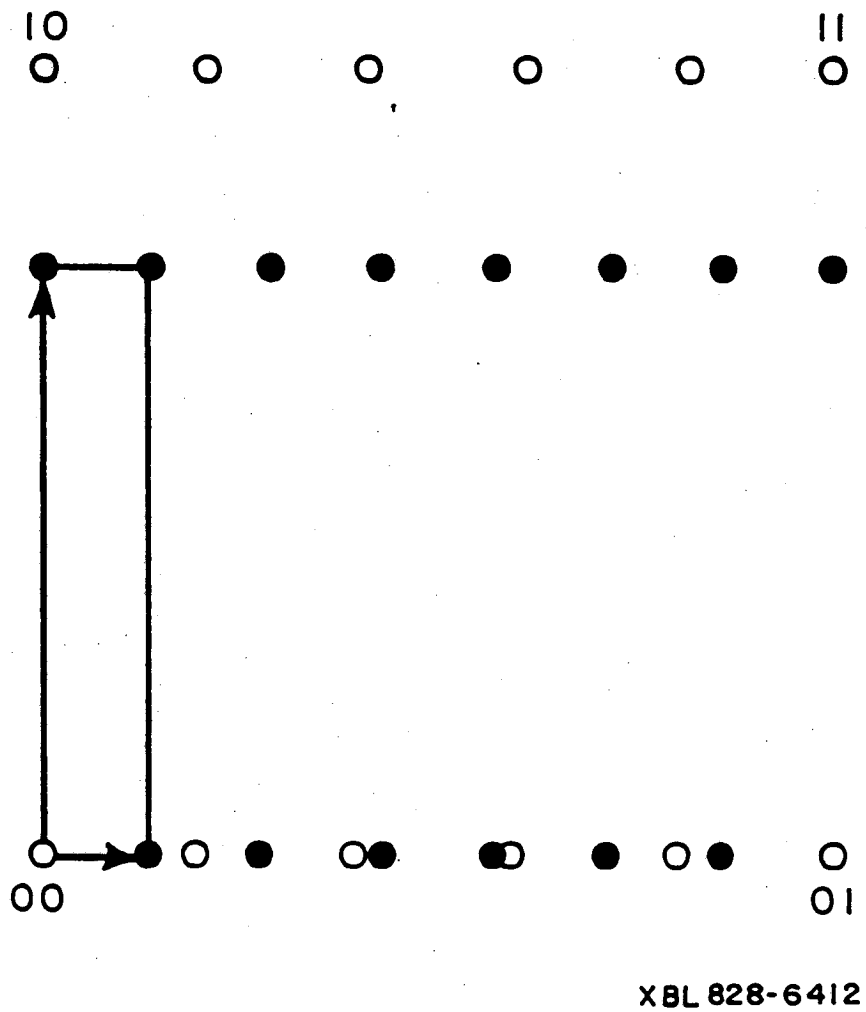

Fig. 4c

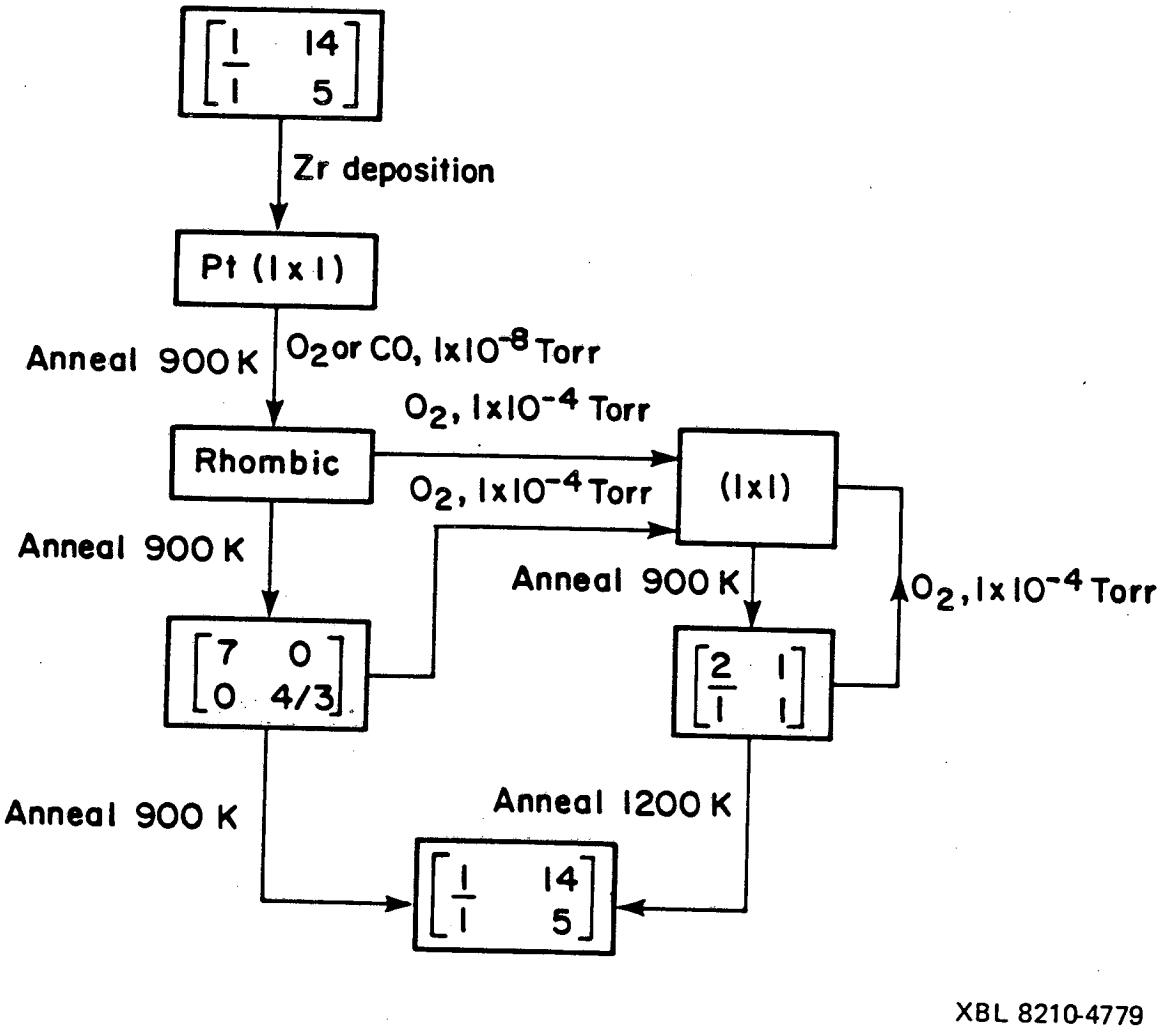

XBL 8210-4779

Fig. 5

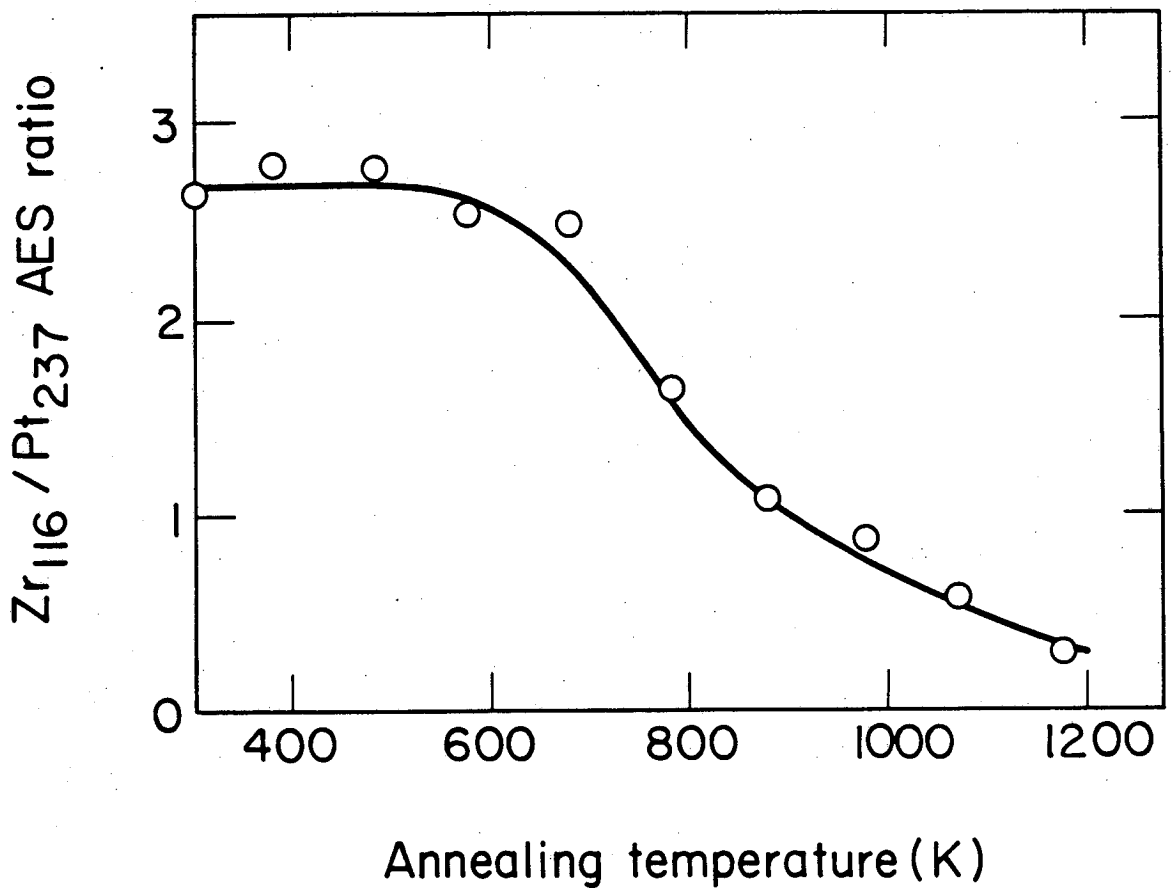

XBL 8210-4778

Fig. 6

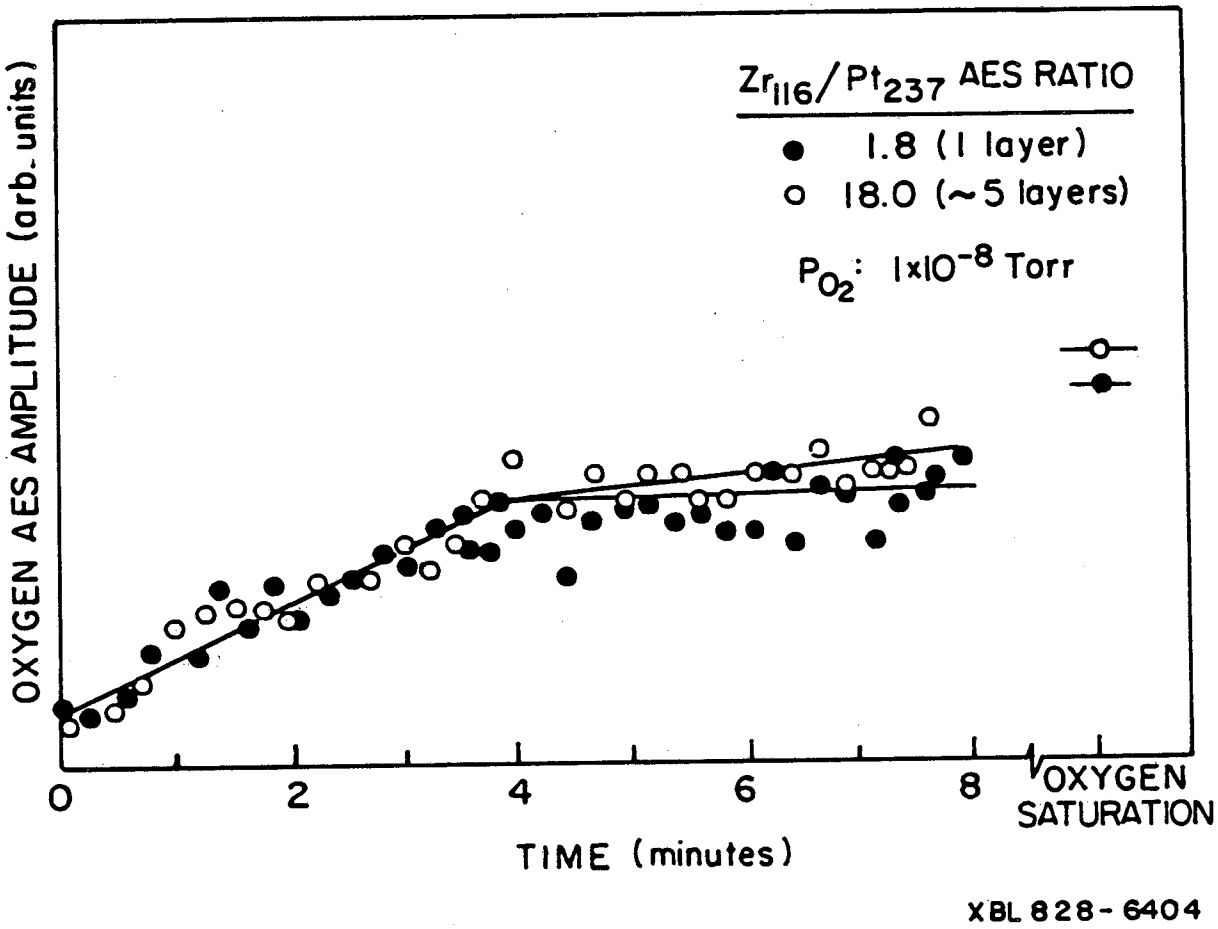

XBL 828-6404

Fig. 7

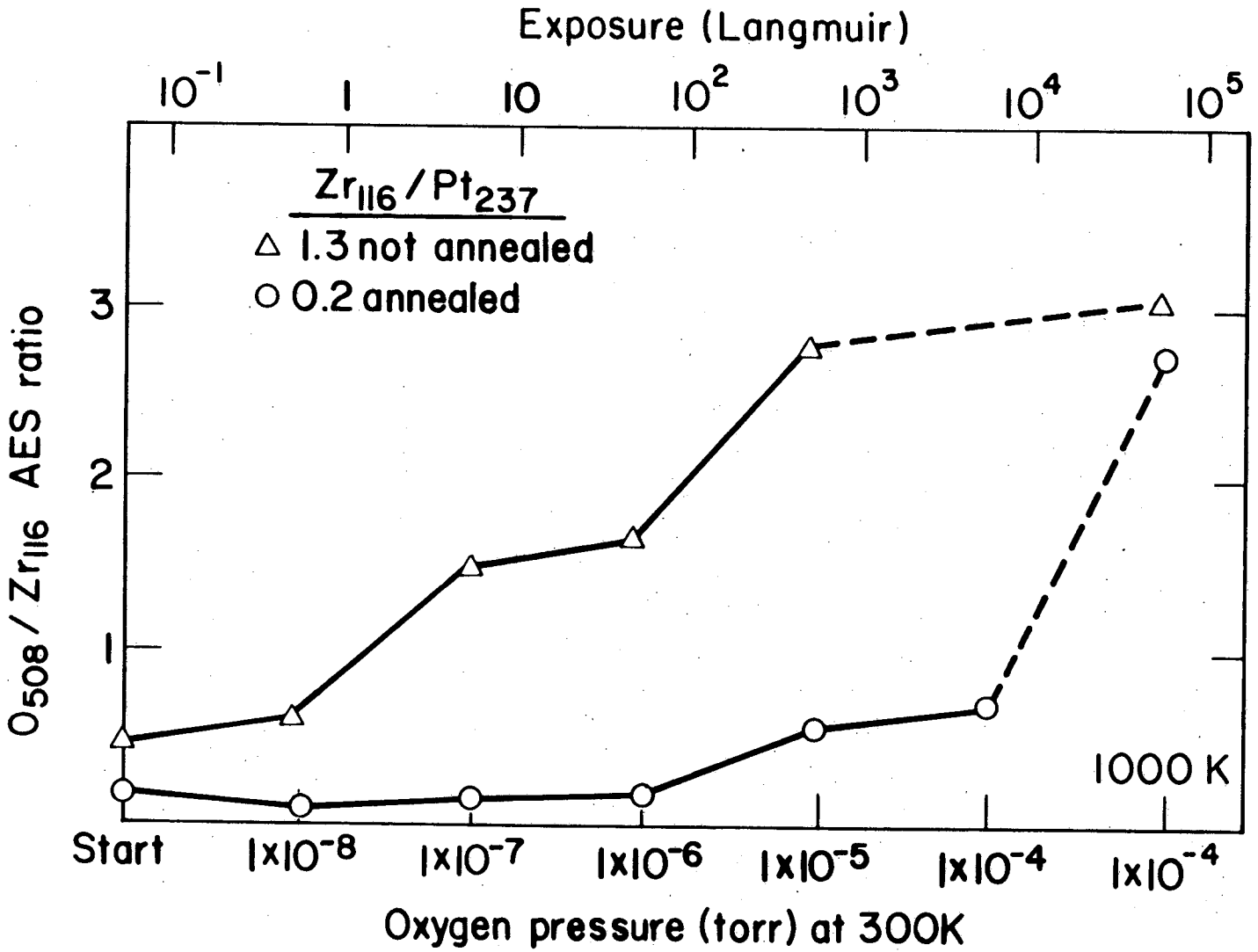

XBL 8210-4777

Fig. 8

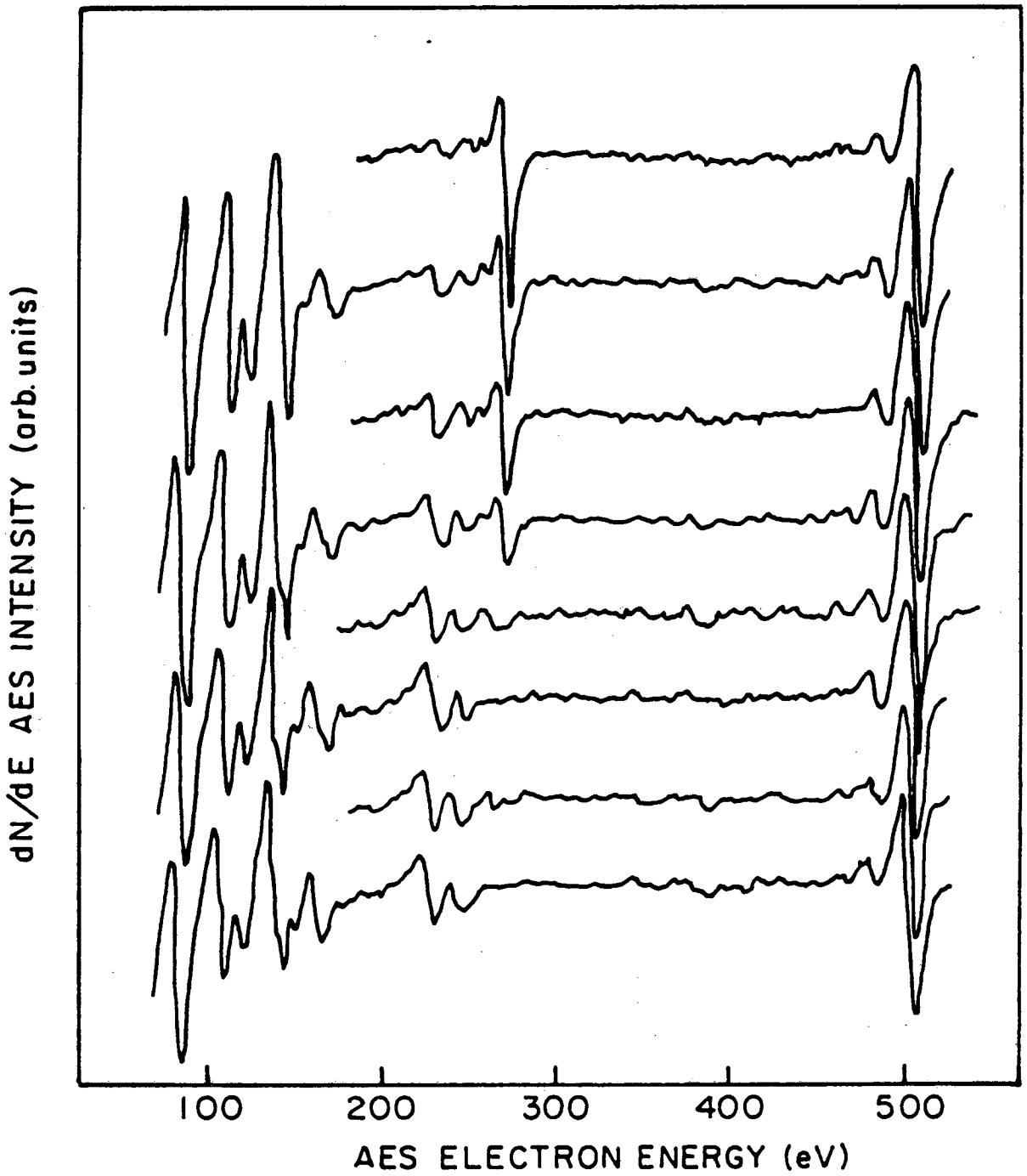

XBL 828-6409

Fig. 9

This report was done with support from the Department of Energy. Any conclusions or opinions expressed in this report represent solely those of the author(s) and not necessarily those of The Regents of the University of California, the Lawrence Berkeley Laboratory or the Department of Energy.

Reference to a company or product name does not imply approval or recommendation of the product by the University of California or the U.S. Department of Energy to the exclusion of others that may be suitable.

TECHNICAL INFORMATION DEPARTMENT
LAWRENCE BERKELEY LABORATORY
UNIVERSITY OF CALIFORNIA
BERKELEY, CALIFORNIA 94720